JOURNAL OF KUFA–PHYSICS
journal.uokufa.edu.iq/index.php/jkp/index | ISSN: 2077–5830

Influence of Annealing Process on Structural and Optical Properties of SnS Thin Films

*** Inass Abdulah Zgair[1]** **Abdulazeez O. Mousa Al-Ogaili[1]** **Khalid Haneen Abass[2]**

[1]*Department of Physics, College of Science, University of Babylon, Babel, Iraq*
[2]*Department of Physics, College of Education for Pure Sciences, University of Babylon, Babel, Iraq.*

*Corresponding Author E-mail: inass.taha.scihigh65@student.uobabylon.edu.iq

ARTICLE INF.

Article history:
Received: 03 JUN., 2023
Revised: 11JUL., 2023
Accepted: 01 AUG., 2023
Available Online: 16 DEC., 2023

Keywords:

Tin Sulfide
Thermal Evaporation
Annealing

ABSTRACT

Thin film technology has helped offer an understanding of the crystalline structure of substances, further to the characteristics of electronic transitions and how they are used effectively in different applications. This research, focused on the effect of the process of annealing on the structural and optical characteristics of tin sulfide (SnS) thin films. The technique of thermal evaporation was used to synthesize the film samples under a vacuum of about 10^{-7} mbar. The coated SnS thin films were annealed at 200 °C and the structural and optical characteristics parameters, such as absorbance and transmittance, as well as optical bandgap and band-tail energies in the range (300–1150) nm, were discussed. Under the influence of the annealing process, the average crystal size changed from 14 nm to 11 nm. The energy gap value increased from 1.53 eV to 1.85 eV, while Urbach energy was seen to reduce from 0.913 eV for fabricated samples to be 0.824 eV after the annealing process.

DOI: https://doi.org/10.31257/2018/JKP/2023/v15.i02.12262

تأثير عملية التلدين على الخصائص التركيبية والبصرية لأغشية ل SnS الرقيقة

ايناس عبدالله زغير طه[1] **عبدالعزيز عبيد موسى العكيلي[1]** **خالد حنين عباس حسن[2]**

[1]قسم الفيزياء, كلية العلوم, جامعة بابل
[2]قسم الفيزياء, كلية التربية للغلوم الصرفة, جامعة بابل

الكلمات المفتاحية:

كبريتيد القصدير
التبخير الحراري
التلدين

الـــخُـــلاصــــة

تقنية الأغشية الرقيقة تساعد في تقديم فهم للبنية البلورية للمادة ، بالإضافة إلى خصائص التحولات الإلكترونية وكيفية استخدامها بفعالية في التطبيقات.في هذا البحث تم دراسة تأثير عملية التلدين على الخصائص التركيبية والبصرية لأغشية كبريتيد القصدير *(SnS)* الرقيقة. حيث تم استخدام تقنية التبخير الحراري لتحضير الاغشية تحت ضغط يبلغ حوالي 10^{-7} ملي بار ، وتم تلدين أغشية *SnS* الرقيقة المحضرة عند 200 درجة مئوية. تمت دراسة الخصائص

التركيبية و البصرية ، مثل الامتصاصية والنفاذية ، بالإضافة إلى فجوة الطاقة البصري وطاقات اورباخ في نطاق(300 إلى 1150) نانومتر. تحت تأثير عملية التلدين ، لوحظ نقصان في معدل الحجم الحبيبي من (14 إلى 11) نانومتر ، وزادت قيمة فجوة الطاقة من (1.53 إلى 1.85) الكترون فولت ، بينما انخفضت طاقة أورباخ من 0.913 الكترون فولت للعينات المصنعة إلى 0.824 إلكترون فولت بعد عملية التلدين.

1. INTRODUCTION

The IV–VI semiconductors groups serve a significant role in the manufacture of photovoltaic devices due to their appropriate features. These include energy band gap, high optical transmittance, and control over electrical characteristics [1,2]. One of these promising material is Tin monosulfide (SnS) which have an appropriate optical characteristic for solar cells owing to the fact that the SnS has a direct band gap of around 1.3 eV, almost identical to the solar radiation optimal value and it has absorption coefficient if about 10^4 cm^{-1} [3-5]. Several effectivetechniques were used in recent years to create SnS thin films, such as chemical bath deposition [6], pulsed laser deposition [7], SILAR [8], pulse electro-deposition [9], sputtering and electron beam evaporation [10]. Rodriguez et al., have coated SnS thin films at Ts=320–396 °C by spray pyrolysis deposition [11]. Zhao et al., were using a technique of atomic layer deposition to fabricate SnS film at temperatures between (80 and 200)°C [12]. Hegde et al., used thermal evaporation to deposit tin sulfide onto glass substrates at 300 °C followed by an annealing process at a range of temperatures from (100 to 300) °C for 2 hours. The average particle size decreased from 265 nm for as-prepared films to 132.8 nm for films annealed at 300°C [13]. Alagarasan *et al.*, fabricated SnS films using vacuum thermal evaporation onto glass substrates at 10^{-5} Torr with various range of substrate temperatures ranging (50 to 200) °C with steps of 50 °C [14]. In this study, SnS film was fabricated with effective, low cost and large area coating using thermal evaporation technique and annealed at 200°C.

2. EXPERIMENT WORK

In this study, Tin Sulfide (SnS) was observed as a powder from Zhengzhou dongyao nano materials Co. LTD/ China company, with nano grain size 50 nm, density 5 g/cm^3, color white, and high purity 99.99 % was placed in a boat of tungsten in order to prepare tin sulphide´s films via thermal evaporation. In this method, a solid substance is heated to its point of evaporation inside a high-vacuum chamber. The substrates are held inverted at the highest point of the chamber, and the material is placed at the bottom, quite on the inside of the boat. After the molecules have evaporated, they make their way from the boat to the substrate, where they nucleate to create a very thin coating [15]. Fig.1. represent the block diagram of thermal evaporation system. The glass substrate that was used for this work of type (citoplus glass) with dimensions (2.5×7.62) cm^2 was placed away from the tungsten boat at 15 cm, and a rate of deposition around (0.3) $nm \cdot s^{-1}$ which represents the ratio of thickness to deposition time while the pressure was $1x10^{-7}$ mbar. The crystalline structure of the samples has been measured by utilizing a (Shimadzu-6000) X-ray diffractometer with Cu Kα (λ = 15,406˚A) radiation. The FESEM device made via (ARYA Electron Optic) company was used to examine the morphology of SnS film. In the range of wavelength 300 – 1200 nm wavelength, a UV-Vis spectrometer (UV-1650 Shimadzu) was employed to measure optical characteristics as a function of wavelength.

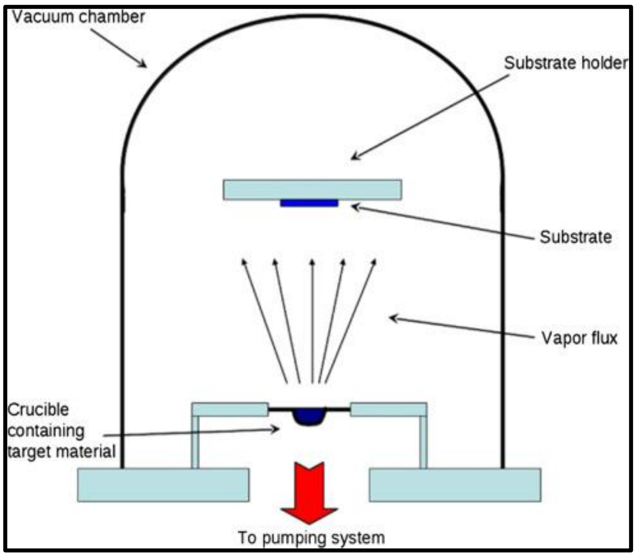

Fig. 1. Thermal evaporation system [15].

3. RESULTS AND DISCUSSION

Fig. 2. Displays the X-ray diffraction patterns of the prepared and annealed films at 200°C for 2h. The figure depicted the poly-crystalline structure of the synthesized films with (Orthorhombic) phase. The distinctive peaks of all SnS thin films have a high degree of concordance with conventional crystallographic data of (JCPDS #00-001-0984) and (JCPDS #01-079-2193. The preferable orientation was seen at 2Θ=28.547° with another main sharp peak belonging to (003) and (102), planes at (2Θ=22.306° and 27.55°), respectively, as well as peaks with less intense at (2Θ=59.06 and 63.843) that belong to (025) and

(008). From the Fig.(2b) there is a clear shifting in the direction of the prominent peaks, which may be caused by the release of intrinsic strain during annealing process [16].

The crystallite size (G) of prepared samples can be obtained using the Scherrer equation [17,18]:

$$G = \frac{K\,\lambda}{\beta\ COS\theta} \qquad (1)$$

Where G is the crystallite size (nm), k is constant with value 0.9, λ denoted to the X-ray wavelength (λ =1:54056 Å), β (rad) represented the full width at half maximum and θ symbolized the Bragg angle .

The Williamson and Smallman's equation can be used to compute the dislocation density (δ), which represents the length of dislocation lines per unit of volume of the crystal [19,20]:

$$\delta = \frac{1}{G^2} \qquad (2)$$

The micro-strain (ε) of the SnS thin films was computed using the following equation [21].

$$\varepsilon = \frac{\beta cos\theta}{4} \qquad (3)$$

The average crystallite size of the preferred orientations had decreased from 14 to 11 after the annealing process. Micro-strain and dislocation density variation are inversely correlated with average crystalline size variation, where it has been reduced while micro-strain and dislocation density have increased as presented in Table (1), and this consequence is opposite to that obtained by R. Balakarthikeyan et al. [22].

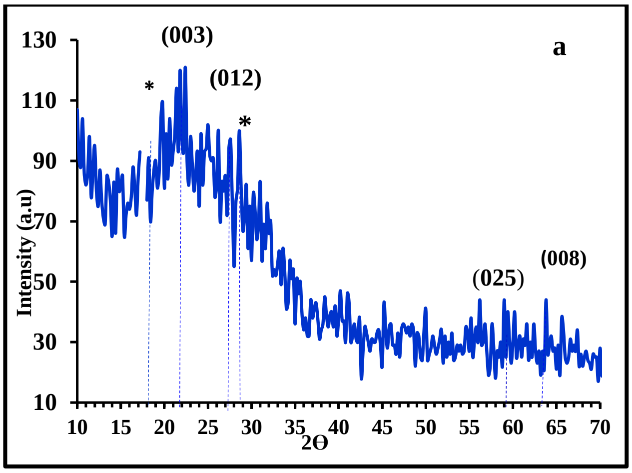

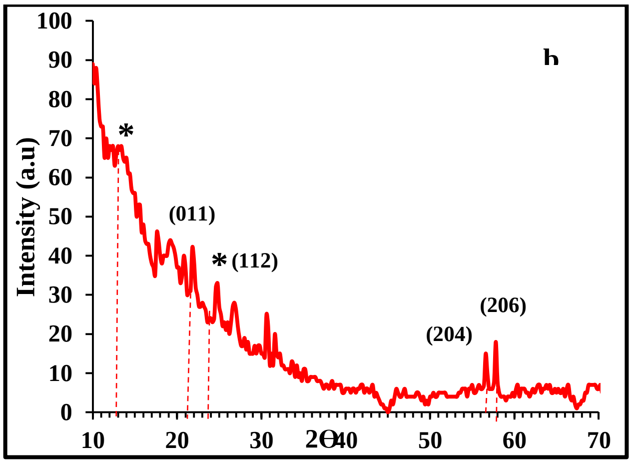

Fig. 2. XRD pattern of SnS/glass thin films : (a) as fabricated and (b) as annealed at Ta= 200°C.

Table (1): Structural parameters of SnS samples as growth and as annealed**.**

Sample	2Θ (deg)	FWHM	(hkl)	Average Crystal Size (nm)	$\delta=1/D^2$	Average micro-strain
SnS thin film as deposited	19.66	0.667	---	14	0.0051	0.1496
	22.30	0.567	(003)			
	27.55	0.567	(102)			
	28.54	0.581	---			
	59.06	0.603	(025)			
	63.843	0.473	(008)			
SnS thin film as annealed	13.49	0.7	-----	11	0.0082	0.1818
	21.92	0.403	(011)			
	24.71	0.586	----			
	26.81	0.986	(112)			
	56.64	0.737	(204)			
	57.76	0.329 0.15948	(206)			

The morphology of SnS thin film can be seen in Fig. 3, where the cross-section of the film surface illustrates that the particles appear elongated onto the film surface are homogeneous, smooth, densely packed, and are pinhole-free.

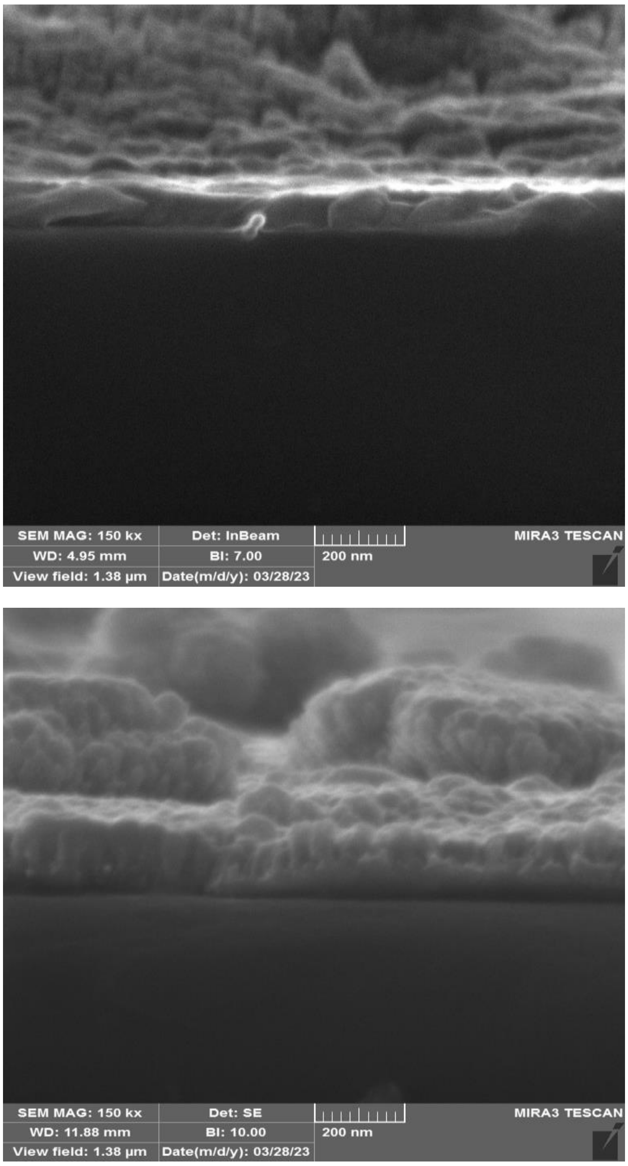

Fig.3. FESEM Images and cross-section of SnS nanofilms: (a) as deposited and (b) as annealed at 200 °C for 2 h.

Fig.4.Illustrates the absorbance curves of as-fabricated and annealed SnS/glass thin films. The absorption edge was shifted toward the lower wavelengths (higher energies) after the annealing process and the value of absorbance can be seen in the UV- region. This behavior is similar to that obtained by Tafti *et al.* when depositing SnS/CdS/glass thin films by the method of thermal evaporation and annealing at 100 to 400 °C, especially at 200 °C [23].

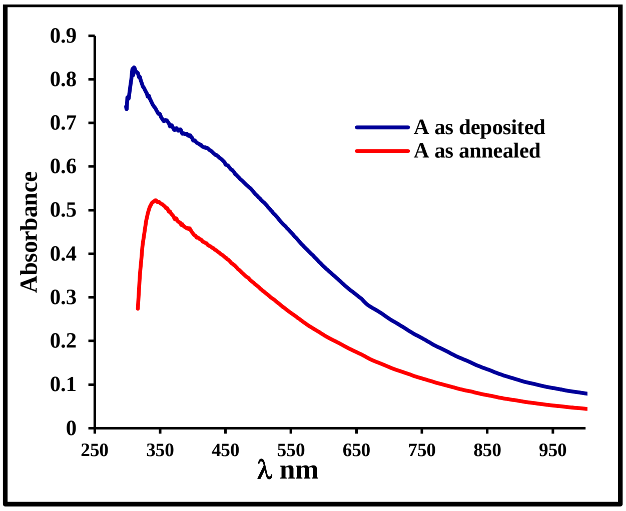

Fig. 4. Absorbance spectra of SnS/glass thin films :as fabricated and annealed at 200˚C.

Fig.5. SnS film spectrum of optical transmission (T%) displayed in range of the wavelength (300–1200) nm. For all films the average of transmittance T% was observed in the UV range and increases from 68% to 85% after annealing process and this consequence closed to obtained via researchers [24,25].

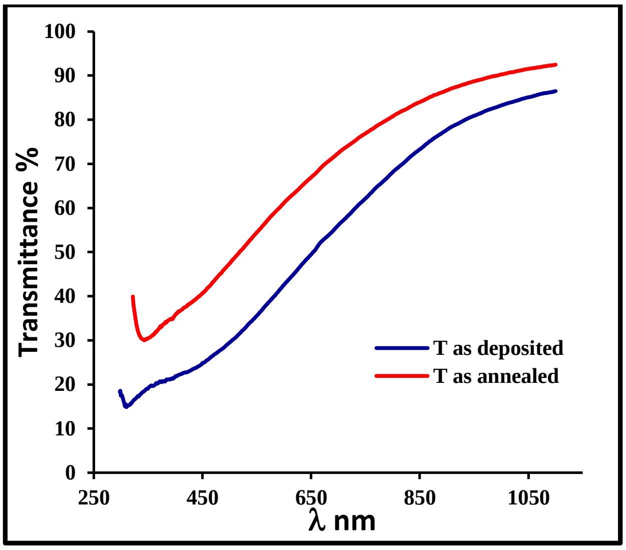

Fig.5.Transmittance spectrum of SnS/glass:as fabricated and as-annealed at 200◦C.

Because of the quantum confinement effect, which is caused by minimizing the crystal size and the dimension of structure a (blue shift) can be seen in this case as well as increasing the transmittance of the thin film [26].

The extinction coefficient represents the amount of light that lost by absorption and scattering per unit distance of the medium. It can be assessed from the following relation [27,28]

$$K = \frac{\alpha\lambda}{4\pi} \qquad (4)$$

Fig.6.Illustrates that the extinction coefficient gradually shifts toward the high energy with an increase in temperature via the process of annealing.

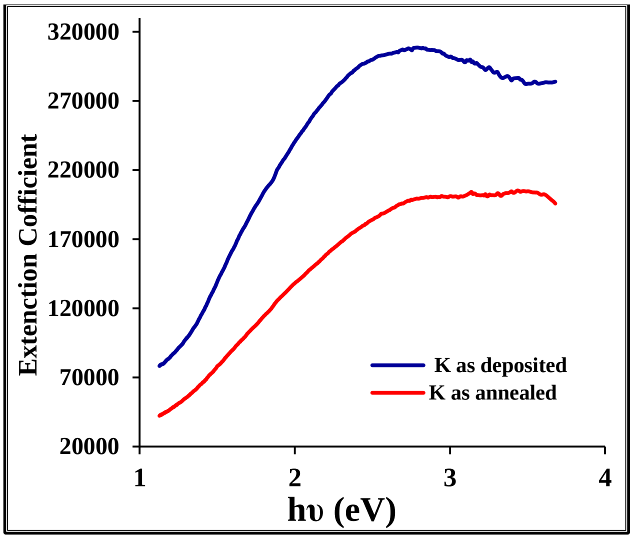

Fig.6.: Extinction coefficient of SnS/glass: before and after the process of annealing.

Fig.7. Displays the direct energy band gap of SnS/glass nanofilms which can be estimated by Tauce formula [29,30].

$$\alpha h\nu = C(h\nu - E_g)^m \qquad (5)$$

The fragmentation of larger grains, which resulted in a reduction in grain size, maybe the reason for the increase in the energy gap value that occurred after the annealing process, which went from 1.53 eV to 1.85 eV and the consequence behavior was nearly close to that obtained by the literatures (Reddy) et al.,[31].

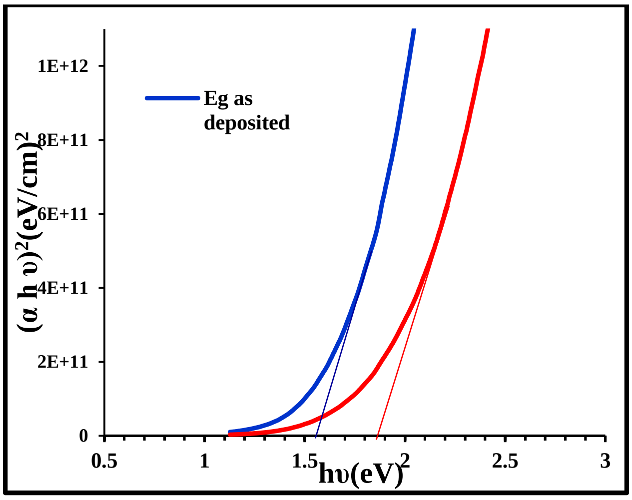

Fig. 7. Energy band gap of SnS/glass thin film as prepared and as-annealed at Ta= 200◦C.

The empirical Urbach´s formula was utilized to estimate the Urbach energy tailing (Eu) of the absorption edge of SnS as follows [32,33].

$$\alpha = \alpha_\circ \exp\frac{h\nu}{E_U} \rightarrow E_U = \left[\frac{d\ln\alpha}{dh\nu}\right]^{-1} \qquad (6)$$

where α denoted to the absorption coefficient, α_0 is a constant, and E_U characterizes the Urbach energy.

SnS thin film samples that have been deposited and annealed have Urbach energies (E_U) of 0.913 eV and 0.824 eV, respectively. As the energy band gap widens as previously revealed, Urbach energy reduced after the annealing process as shown in Fig.8. which may be caused by a decrease in localized states in the band gap, this behavior is similar to that gotten by Kherchachi et al., [34].

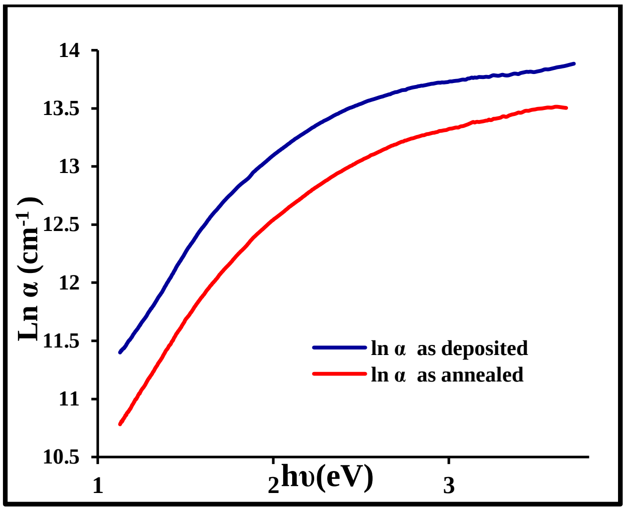

Fig.8. Urbach of SnS/glass thin film: (a)as deposited and (b)as-annealed at Ta= 200◦C.

The following formulae can be applied to determine the volume (VELF) and surface energy loss functions (SELF), which characterize the energy lost as electrons move within a material or across its surface. [35,36]:

$$VELF = \frac{\varepsilon_i}{(\varepsilon_r + 1)^2 + \varepsilon_i^2} \qquad (7)$$

$$SELF = \frac{\varepsilon_i}{\varepsilon_r^2 + \varepsilon_i^2} \qquad (8)$$

Where real and imaginary portions of the dielectric constant are denoted by (εr) and (εi).

As seen in Fig.9. the absorption edge has moved towards a higher energy after annealing, whereas VELF has shifted towards a lower energy.

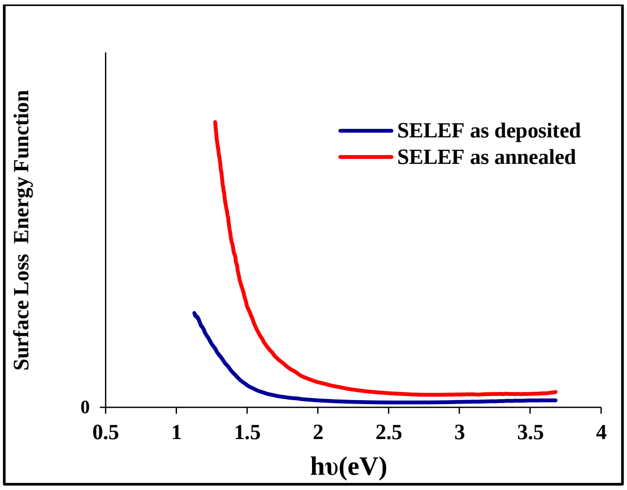

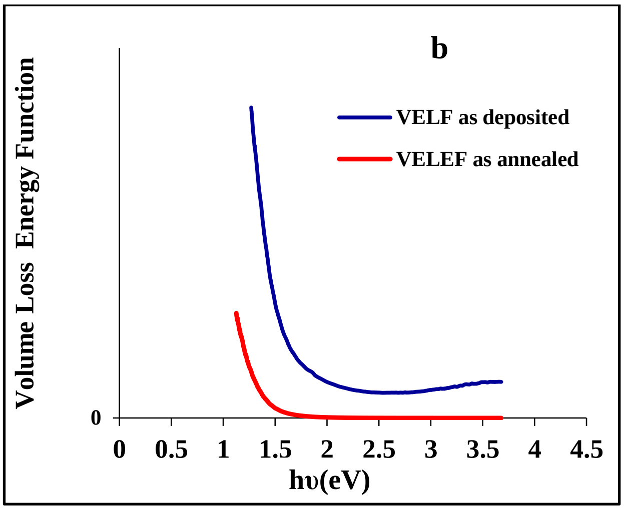

Fig. 9.: (a) SELF and (b) VELF of SnS Thin films.

4. CONCLUSIONS

In this paper, thermal evaporation technique was utilized to deposit SnS thin films onto a glass substrate and annealed at temperatures of 200 ^{o}C. The X-ray diffraction measurement reveals that SnS films have an orthorhombic phase with polycrystalline structure and there is a reduction in average crystal size after the annealing process. Image of FESEM shows the morphology of SnS thin film appears relatively plated regularly and has uniform distribution. The optical transmission of the coating samples is greater than 85% in the visible spectrum, and the energy band gap was increased from 1.53 eV to 1.85 eV after the annealing process while Urbach energy decreased. In light of the results, it's possible to conclude that the SnS thin films characteristics are appropriate for use in solar cells

5. REFERENCES

[1] J. Johny, S. Sepulved-Guzman, B. Krishnan, D.A. Avellaneda, J.A. Aguilar Martinez, M.R. Anantharaman and S. Shaji,, Tin sulfide: Reduced graphene oxide nanocomposites for photovoltaic and electrochemical applications, Solar Energy Materials and Solar Cells, Vol. 189, 2019, pp. 53–62.

[2] S. John , M. Francis, A. P. R. Mary , V. Geetha, Influence of annealing on the properties of chemically prepared SnS thin films, Chalcogenide Letters, Vol.20, No.5, (2023), pp.315-323.

[3] M. Messaoudi, M. S. Aida, N. ATTAF, A. Bebbouche, S. Satta, Influence of Sulphur Molar Concentration on Structural and Optical Properties of Tin Sulphide Tin Films, Chalcogenide Letters, Vol. 17, No. 5, 2020, pp. 223 – 228.

[4] S. Kancharla and D. K. Kaushik, Optimization of Electrical and Optical Properties of Tin Sulfide for Thin Film Photovoltaics using SCAPS, Journal of Physics: Conference Series, Vol. 1531, 2020, pp.1-7.

[5] P.A. Nwofe and M. Sugiyama: Tuning and enhancing performance in RF sputtered SnS thin film solar cells, De Gruyter, Vol,76, No.2, 2021, pp. 181–195.

[6] E. Sarica, Investigation of spray pyrolyzed cubic structured Cu doped SnS films", Phosphorus, Sulfur, and Silicon and the Related Elements, , Vol. 196, No. 12, , 2021, pp. 1103–1108

[7] K. Ungeheue, K. W. Marszalek, M. Mitura-Nowak, P. Jelen, M. Perzanowski,M. Marszalek and M. Sitarz, Cuprous Oxide Thin Films Implanted with Chromium Ions Optical and Physical Properties Studies, International, Journal of Molecular Sciences, Vol. (2022), pp.2-13.

[8] R. Kihal, H. Rahal, A. M. Affoune, and M. Ghers, Electrodeposition of SnS Thin film Solar Cells in the Presence

of Sodium Citrate, J. Electrochem. Sci. Technol., Vol. 8,No.3, 2017, pp. 206-214.

[9] F. Jiang, H. Shen, W. Wang, and L.Zhang, Preparation of SnS Film by Sulfurization and SnS/a-Si Heterojunction Solar Cells, Journal of The Electrochemical Society, Vol. 159,No. 3, 2012, pp. H235-H238.

[10] I. Suzuki, S. Kawanishi, T. Omata and H.Yanagi, Current status of n-type SnS: paving the way for SnS homojunction solar cells, Journal of Physics: Energy, Vol. 4, No. 4, 2022 ,pp.1-13.

[11] E. Guneri, F. Gode, C. Ulutas, F. Kirmizigul, G. Altindemir and C. Gumus, Properties of P-type SnS Thin Films Prepared by Chemical Bath Deposition, Chalcogenide Letters Vol. 7, No. 12, 2010, pp.685-694.

[12] X. Zhao, L.M. Davis, X. Lou, S. B. Kim, S. Uliˇcan, A.Jayaraman, C.Yang, L.T. Schelhas, and R. Gordon, Study of the Crystal Structure of SnS Thin Films by Atomic Layer Deposition, AIP Advances, Vol.11, 2021, pp.1-6.

[13] S.S. Hegde, A.G. Kunjomana, P. Murahari , B.K. Prasad and K. Ramesh, Vacuum Annealed Tin Sulfide (SnS) Thin Films for Solar Cell Applications, Surfaces and Interfaces,Vol.10, 2018, pp. 78-84.

[14] D. Alagarasan, S. Varadharajaperumal , K. D. A. Kumar, R. Naik, S. Umrao, M. Shakir, S. AIFaify and R. Ganesan, Influence of Nanostructured SnS Thin Films for Visible Light Photo Detection, Optical Materials, Vol. 121, 2021, p.111489.

[15] K.L. Chopra, Thin Film Devices Application, Plenum Press, New York, 1983.

[16] T. Daniel, U.Uno, K.Isah, U. Ahmadu ,Tuning of SnS Thin Film Conductivity on Annealing in an Open Air Environment for Transistor Application, East Eur. J. Phys.,Vol. 2, 2020, pp. 94-103.

[17] A.N. Tuama, K. H. Abass and Mohd Arif Agam, Fabrication and Characterization of Cu2O:Ag/Si Solar Cell Via Thermal Evaporation Technique, International Journal of Nanoelectronics and Materials Vol. 13, No. 3, 2020,pp. 601-614.

[18] S.M. Thahab, A.H.O. Alkhayatt and Salah M. Saleh, The optical properties of CdxZn1−x S thin films on glass substrate prepared by spray pyrolysis method, Optik,Vol.125,2014 ,pp. 5112–5115.

[19] A.H. Omran Alkhayatt and S. K. Hussian, Fluorine dopant concentration effect on the structural and optical properties of spray deposited nanocrystalline ZnO thin films, Surfaces and Interfaces ,Vol.8,2017 ,pp. 176–181.

[20] K. R. Kadhim and R.Y. Mohammed, Effect of Annealing Time on Structure, Morphology, and Optical Properties of Nanostructured CdO Thin Films Prepared by CBD Technique, Crystals, Vol.12, No.1315,2022, pp.1-18.

[21] A. Doula, R. Bensaha and O. Beldjebli, Structural, Optical and Photocatalytic Properties of Ba-Doped TiO2 Thin Films, ACTA PHYSICA POLONICA A No. 5 Vol. 140,2021, pp.421-426.

[22] R. Balakarthikeyan , A. Santhanam , A. Khan, A. M. El-Toni , A. A. Ansari , A. Imran, M. Shkir and S. AlFaify, Performance Analysis of SnS Thin Films Fabricated Using Thermal Evaporation Technique for Photodetector Applications, Optik International Journal for Light and Electron Optics ,Vol. 244, 2021, pp. 1-11.

[23] Z. D. Tafti, M. B. Zarandi, H. A. Bioki, Thermal Annealing Influence over Optical Properties of Thermally Evaporated SnS/ CdS Bilayer Thin Films, Journal of Opto-electronical Nanostructures, Vol. 4, No.1, 2019, pp. 87-98.

[24] J.I Onwuemeka, F.M. Ezike, N.C Nwulu, The Effect of Annealing Temperature and Time on the Optical Properties of SnS Thin Films Prepared by Chemical Bath Deposition, International Journal for Innovation Education and Research Vol. 1 No. 2, 2013, pp. 96-104.

[25] T. R. Kishore Bhat, K. Jeganath, S. D. George, and Y. Raviprakash, Annealing-induced phase conversion on spray pyrolyzed cubic-SnS thin films, J Mater Sci: Mater Electron , Vol. 34,No. 747, 2023, pp. 2-4.

[26] G. Wisz, P. Sawicka-Chudy, P. Potera, M. Sibiński, R. Yavorskyi, Ł. Głowa, B. Cieniek and M. Cholewa, Morphology, Composition, Structure and Optical Properties of Thermally Annealed Cu2O Thin Films Prepared by Reactive DC Sputtering Method, Molecular Crystals and Liquid Crystals, Vol. 672, No.1, 2018, pp. 81–91.

[27] S. M. Sze and Kwok K. Ng, Physics of Semiconductor Devices Third Edition, John Wiley & Sons, Inc., 2007.

[28] E. D. Palik, Handbook of Optical Constants of Solids. II, Academic Press, California 1998.

[29] J. Tauc, Amorphous and Liquid Semiconductors, Plenum Press, USA, 1974.

[30] K. H. Abass and N. H. Obaid, 0.006wt.%Ag-Doped Sb2O3 Nanofilms with Various Thickness: Morphological and optical properties, IOP Conf. Series: Journal of Physics: Conf.Series Vol. 1294, 2019, p. 022005.

[31] T. Srinivasa Reddy, B. Hemanth Kumar and M.C. Santhhosh Kumar, Effect of Annealing on the optical properties and photoconductivity of SnS thin film, AIP Conference Proceedings, Vol. 1832, 2017, pp.1-3.

[32] M. kumar, Optical Analysis of Spray Pyrolysis Synthesized CdS Thin Films for Solar Cell Applications, International Advanced Research Journal in Science, Engineering and Technology, Vol. 10, Issue 6, 2023, pp.30-34.

[33] M. Haj Lakhdar, B. Ouni and M. Amlouk, Thickness effect on the structural and optical constants of stibnite thin films prepared by sulfidation annealing of antimony films, Optik ,Vol.125, 2014, pp. 2295–2301.

[34] I. B. Kherchachi., A. Attaf, H. Saidi, A. Bouhdjer, H. Bendjedidi, Y. Benkhetta, and R. Azizi, Structural, optical and electrical properties of SnxSy thin films grown by spray ultrasonic, Journal of Semiconductors, Vol. 37, No. 3, 2016, pp.1-6.

[35] K. H. Abass, M. H. Shinen and A.F. Alkaim, Preparation of TiO2 nanolayers via. Sol-Gel Method

and Study the Optoelectronic Properties as Solar Cell Applications, Journal of Engineering and Applied Sciences, Vol. 13, No.22, 2018, pp.9631-9637.

[36] Z.M. Jawad and K. H. Abass, Fabrication and Study the Optical Properties and Dispersion Parameters of PVA/PAAm with CuNW Additive, Neuro Quantology, Vol. 20, No.2, 2022, pp. 87-95.